

Unconditional preparation of entanglement between atoms in cascaded optical cavities

Stephen Clark, Amy Peng, Mile Gu, and Scott Parkins

Department of Physics, University of Auckland, Private Bag 92019, Auckland, New Zealand.

(Dated: November 11, 2018)

We propose a scheme to unconditionally entangle the internal states of atoms trapped in separate high finesse optical cavities. The scheme uses the technique of quantum reservoir engineering in a cascaded cavity QED setting, and for ideal (lossless) coupling between the cavities generates an entangled *pure* state. Highly entangled states are also shown to be possible for realizable cavity QED parameters and with nonideal coupling.

PACS numbers: 03.65.Ud, 03.67.-a, 42.50.-p

Cold trapped atoms and quantum light fields are promising candidates for the realization of quantum computing and quantum communication protocols [1, 2], with long-lived atomic states (electronic or motional) constituting quantum registers, upon which (local) quantum logic operations can be performed, and light fields providing a means of distributing quantum information and entanglement between different nodes in a network of registers [3]. The workability of such atom-light networks will depend heavily on the extent to which propagating light fields can reliably transfer quantum states and/or establish quantum entanglement between atoms at different nodes of the network.

In the context of entanglement preparation between atoms at separate nodes, a variety of schemes have been proposed recently. Based on their operating principles, these schemes can be grouped loosely as follows: (i) “Local” entanglement, prepared by some means between atoms at one node, is transferred, via carefully-controlled quantum state-transferring light pulses, from a subset of the entangled atoms to atoms at a distant node [3, 4]. (ii) Quantum-correlated light fields, produced, e.g., by nondegenerate parametric downconversion, interact with separate atoms in such a way as to transfer some of their properties to, and thereby entangle, the atoms [5, 6, 7, 8, 9, 10]. (iii) Measurements (e.g., single-photon detections or homodyne detection over some interval) are made on superpositions of light fields emanating from separate atomic samples, or on a probe light field that has interacted in a prescribed way with different samples. Indistinguishability in the measurement conditionally projects the atomic systems into an entangled state [11, 12, 13, 14, 15, 16, 17, 18, 19, 20].

Here we propose a scheme for preparing distributed atomic entanglement that is quite distinct from those listed above. While it employs cascaded cavity QED systems (as, e.g., in [3, 4]), it does not require initial local entanglement between atoms or tailored optical pulses, nor does it involve separate nonclassical light sources or projective measurements. The entangled atomic state is prepared *unconditionally* and under *steady state* conditions. Furthermore, the degree of entanglement (and also the mixedness) of the state is adjustable through varia-

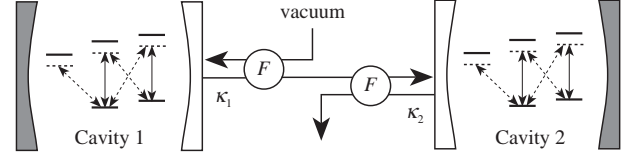


FIG. 1: Cascaded cavities, each containing a trapped atom. A unidirectional coupling between the cavities is achieved using Faraday isolators (F). The (one-sided) cavities have field decay rates κ_1 and κ_2 .

tion of certain tunable system parameters (i.e., Raman coupling strengths), and, for ideal transmission of light between cavities, a *pure* entangled state can be prepared.

Our scheme employs quantum reservoir engineering [21] in a cavity QED setting [22]. Two high-finesse optical cavities, each containing one tightly confined atom, are arranged in a cascaded configuration with a unidirectional coupling from cavity 1 to cavity 2 (Fig. 1). Both cavities are taken to have the same resonant frequency ω_{cav} and their individual field decay rates are κ_1 and κ_2 . Inefficiencies and losses in the coupling between the two cavities are modelled by a real parameter ϵ , where $0 \leq \epsilon \leq 1$ and ideal coupling corresponds to $\epsilon = 1$.

Each atom has two stable ground states, $|0\rangle$ and $|1\rangle$ (the qubit states). The cavity field and two auxiliary laser fields drive two separate Raman transitions between these states (Fig. 2). In particular, transitions $|1\rangle \leftrightarrow |r\rangle$ and $|0\rangle \leftrightarrow |s\rangle$ are driven by detuned laser fields with (complex) Rabi frequencies Ω_r and Ω_s , while the transitions $|0\rangle \leftrightarrow |r\rangle$ and $|1\rangle \leftrightarrow |s\rangle$ are strongly coupled to the cavity mode, with coupling strengths g_r and g_s . Detunings of the fields from the excited states $|r\rangle$ and $|s\rangle$ are Δ_r and Δ_s . A fifth state $|t\rangle$ is virtually excited from $|0\rangle$ by another strongly detuned laser field, adding an additional ac-Stark shift to the state $|0\rangle$.

The master equation for the total system density operator ρ_T is (taking $\hbar = 1$)

$$\dot{\rho}_T = -i[H, \rho_T] + \mathcal{L}_{\text{cav}}\rho_T + \mathcal{L}_{\text{spon}}\rho_T, \quad (1)$$

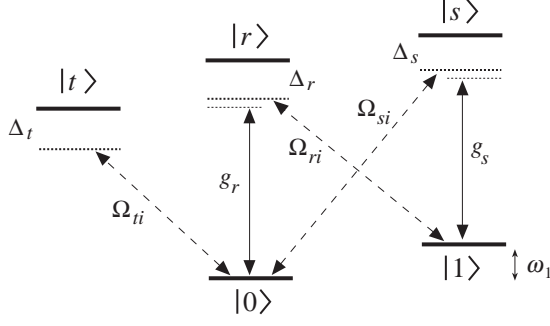


FIG. 2: Level scheme for each atom. The excited states have energies $\hbar\omega_j$ ($j = r, s, t$). Such an atomic configuration could be realized, e.g., with alkali atoms, where $|0\rangle$ and $|1\rangle$ are different ground-state sublevels. Note also that $|r\rangle$ and $|s\rangle$ can be the same level, provided the two Raman channels remain distinct (which would require $\omega_1 \neq 0$). Apart from Ω_{ri} , Ω_{si} and Ω_{ti} , we assume, for simplicity, that all other parameters are the same for each atom.

where $H = H_{\text{cav}} + H_{\text{at}} + H_{\text{int}}$, with

$$H_{\text{cav}} = \sum_{i=1,2} \omega_{\text{cav}} a_i^\dagger a_i, \quad (2)$$

$$H_{\text{at}} = \sum_{i=1,2} \{ \omega_r |r_i\rangle \langle r_i| + \omega_s |s_i\rangle \langle s_i| + \omega_t |t_i\rangle \langle t_i| + \omega_1 |1_i\rangle \langle 1_i| + [(\Omega_{ri}/2)e^{-i\omega_{Lr}t} |r_i\rangle \langle 1_i| + \text{H.c.}] + [(\Omega_{si}/2)e^{-i\omega_{Ls}t} |s_i\rangle \langle 0_i| + \text{H.c.}] + [(\Omega_{ti}/2)e^{-i\omega_{Lt}t} |t_i\rangle \langle 0_i| + \text{H.c.}] \}, \quad (3)$$

$$H_{\text{int}} = \sum_{i=1,2} (g_r |r_i\rangle \langle 0_i| a_i + g_s |s_i\rangle \langle 1_i| a_i + \text{H.c.}), \quad (4)$$

(H.c. denotes Hermitian conjugate) and

$$\mathcal{L}_{\text{cav}}\rho_{\text{T}} = \sum_{i=1,2} \kappa_i \left(2a_i\rho_{\text{T}}a_i^\dagger - a_i^\dagger a_i\rho_{\text{T}} - \rho_{\text{T}}a_i^\dagger a_i \right) - 2\sqrt{\epsilon\kappa_1\kappa_2} \left([a_2^\dagger, a_1\rho_{\text{T}}] + [\rho_{\text{T}}a_1^\dagger, a_2] \right). \quad (5)$$

Here, a_i is the cavity mode annihilation operator for cavity i , ω_{Lj} ($j \in \{r, s, t\}$) denote the laser frequencies, and the term $\mathcal{L}_{\text{spon}}\rho_{\text{T}}$ describes atomic spontaneous emission. The term $\mathcal{L}_{\text{cav}}\rho_{\text{T}}$ describes damping of the cavity modes through their output mirrors, plus the unidirectional coupling from cavity 1 to cavity 2 [23].

Assuming large detunings of the fields from the excited atomic states (i.e., $|\Delta_j| \gg |\Omega_{ji}|$, $g_{r,s}$, κ_i , γ_j , where γ_j is the linewidth of state $|j\rangle$), we can adiabatically eliminate these states, and neglect atomic spontaneous emission, to obtain a simplified model of the system in the form of a reduced master equation for a pair of effective two-level atoms (states $|0\rangle$ and $|1\rangle$) coupled to the cavity modes.

This reduced system is characterized by the parameters

$$\beta_{ki} = \frac{g_k\Omega_{ki}}{2\Delta_k}, \quad \alpha_{ji} = \frac{|\Omega_{ji}|^2}{4\Delta_j}, \quad \eta_k = \frac{g_k^2}{\Delta_k}, \quad (6)$$

where $k \in \{r, s\}$, $i \in \{1, 2\}$, and $j \in \{r, s, t\}$; β_{ki} are Raman coupling rates, while α_{ji} and η_k correspond to laser- and cavity-induced atomic level shifts, respectively.

To further reduce the model, we assume the “bad-cavity” limit: $\kappa_i \gg |\beta_{ki}|, |\eta_k|$. This allows us to adiabatically eliminate the cavity mode to give a master equation for the atomic density matrix ρ :

$$\dot{\rho} = \sum_{i=1,2} \left(2R_i\rho R_i^\dagger - R_i^\dagger R_i\rho - \rho R_i^\dagger R_i \right) - 2\sqrt{\epsilon} \left([R_1\rho, R_2^\dagger] + [R_2, \rho R_1^\dagger] \right), \quad (7)$$

where $R_i = (\beta_{ri}|0_i\rangle\langle 1_i| + \beta_{si}|1_i\rangle\langle 0_i|)/\sqrt{\kappa_i}$.

The first line of (7) describes the separate interaction of each atom with an effective squeezed reservoir [22], while the second line describes a unidirectional coupling between the atoms. As we show below, this combination of squeezing and coupling facilitates the preparation of an entangled steady state of the atoms.

Note that the derivation of (7) also requires that the phase of the effective two-level system remains constant with respect to the phase difference between Ω_{ri} and Ω_{si} , i.e., the two-level atomic systems and squeezed reservoirs must be “resonant” with each other. Under conditions of Raman resonance ($\omega_{\text{cav}} - \omega_{Lr} = \omega_{Ls} - \omega_{\text{cav}} = \omega_1$), this requirement leads to the condition

$$\alpha_{ri} - \alpha_{si} - \alpha_{ti} = 0. \quad (8)$$

It is to satisfy this condition while retaining flexibility in our choices of Ω_{ri} , Ω_{si} and $\Delta_{r,s}$ that we use the additional transition $|0\rangle \leftrightarrow |t\rangle$. The level shift α_{ti} provides an extra degree of freedom with which to satisfy (8).

If the atoms are driven such that $\beta_{r1}/\sqrt{\kappa_1} = \beta_{r2}/\sqrt{\kappa_2} = a$ and $\beta_{s1}/\sqrt{\kappa_1} = \beta_{s2}/\sqrt{\kappa_2} = b$ then an analytic steady-state solution of (7) can be obtained as

$$\rho_{\text{ss}} = \begin{pmatrix} \rho_{11} & 0 & 0 & \rho_{14} \\ 0 & \rho_{22} & \rho_{23} & 0 \\ 0 & \rho_{23}^* & \rho_{33} & 0 \\ \rho_{14}^* & 0 & 0 & \rho_{44} \end{pmatrix}, \quad (9)$$

in the basis $\{|1_11_2\rangle, |1_10_2\rangle, |0_11_2\rangle, |0_10_2\rangle\}$, where

$$\begin{aligned} \rho_{11} &= (|b|^6 + (1 + \epsilon - 4\epsilon^2)|a|^2|b|^4 + \epsilon|b|^2|a|^4)/D, \\ \rho_{22} &= |a|^2|b|^2(1 - \epsilon)(|a|^2 + (1 + 4\epsilon)|b|^2)/D, \\ \rho_{33} &= |a|^2|b|^2(1 - \epsilon)(|b|^2 + (1 + 4\epsilon)|a|^2)/D, \\ \rho_{44} &= (|a|^6 + \epsilon|a|^2|b|^4 + (1 + \epsilon - 4\epsilon^2)|b|^2|a|^4)/D, \\ \rho_{14} &= \sqrt{\epsilon}a^*b(|a|^4 + (2 - 4\epsilon)|a|^2|b|^2 + |b|^4)/D, \\ \rho_{23} &= 2\sqrt{\epsilon}(1 - \epsilon)|a|^2|b|^2(|a|^2 + |b|^2)/D, \end{aligned} \quad (10)$$

and

$$D = (|a|^4 + |b|^4 + 2(1 + 2\epsilon - 4\epsilon^2)|a|^2|b|^2)(|a|^2 + |b|^2).$$

In general, ρ_{ss} describes an entangled mixed state, but for the case of ideal coupling between cavities ($\epsilon = 1$) we obtain the *pure state* $\rho_{ss} = |\psi\rangle\langle\psi|$, where

$$|\psi\rangle = \frac{a|0_10_2\rangle + b|1_11_2\rangle}{\sqrt{|a|^2 + |b|^2}}. \quad (11)$$

Note that the generation of this pure state coincides with a complete absence of photons in the output field from cavity 2, i.e., the cascaded system as a whole is prepared in a *dark*, or *decoherence-free* state.

The state (11) approximates the maximally-entangled Bell states $|\phi^\pm\rangle = (|0_10_2\rangle \pm |1_11_2\rangle)/\sqrt{2}$ in the limit that $a \simeq \pm b$. The Bell states $|\psi^\pm\rangle = (|0_11_2\rangle \pm |1_10_2\rangle)/\sqrt{2}$ may be approximated in the steady state in the same limits simply by choosing $\beta_{r1}/\sqrt{\kappa_1} = \beta_{s2}/\sqrt{\kappa_2} = a$ and $\beta_{s1}/\sqrt{\kappa_1} = \beta_{r2}/\sqrt{\kappa_2} = b$.

To gauge the performance of the scheme under more general conditions, we have performed a variety of numerical simulations taking into account the dynamics of the cavity mode, imperfect coupling between the cavities, and the effects of atomic spontaneous emission. To quantify the degree to which the scheme generates a maximally entangled state, we use the measure of fidelity (maximal singlet fraction), for which an analytic form exists in the case of two qubits [24].

The evolution of the atoms (each prepared initially in the state $|0\rangle$) towards a highly entangled state is shown in Fig. 3 in a plot of fidelity against time, for several values of the ratio a/b and for a non-unit coupling efficiency ϵ . The cavity-QED parameters (g, κ, γ) used are taken from a recent experiment [25]; for simplicity, we assume $g_r = g_s = g$. The solid lines are derived from solutions to (7), while the dashed lines are derived from a more complete model including both cavity dynamics and the effects of atomic spontaneous emission from the three excited levels $|r_i\rangle$, $|s_i\rangle$ and $|t_i\rangle$. (We assume equal branching ratios where two different decay channels are possible, e.g., $|r_i\rangle \rightarrow |0_i\rangle$ and $|r_i\rangle \rightarrow |1_i\rangle$.) With the cavity dynamics included in the model, one finds that cavity-induced level shifts (proportional to $\eta_{r,s}$) can play an appreciable role; in particular, when they are not substantially less than κ . These shifts can be compensated for, and the fidelity of the prepared state optimized, by choosing $\eta_r = \eta_s \equiv \eta$, $\omega_{\text{cav}} = \frac{1}{2}(\omega_{Ls} + \omega_{Lr}) - \eta$, and $\alpha_{ri} - \alpha_{si} - \alpha_{ti} = \frac{1}{2}(\omega_{Ls} - \omega_{Lr}) - \omega_1$, as we do for the results presented in Figs. 3–5.

Returning to Fig. 3, we note first the slowing-down of the evolution towards the steady state as the ratio a/b approaches unity. This behavior is characteristic of atomic evolution in a squeezed reservoir as the degree of squeezing increases [22], which here corresponds to

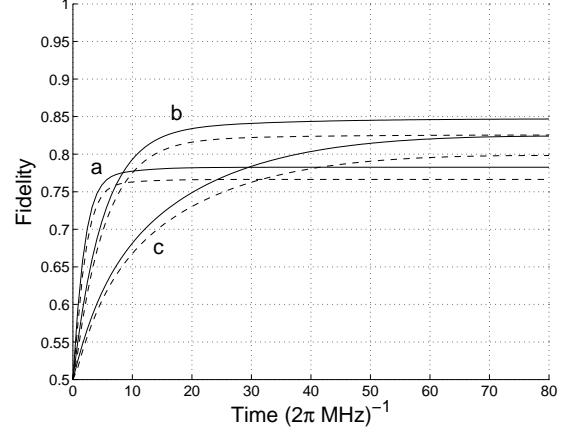


FIG. 3: Fidelity (maximal overlap with a maximally entangled state) versus time for $(g, \kappa, \gamma, \Delta, \Omega_s)/2\pi = (110, 14.2, 5.2, 8000, 100)$ MHz, $\epsilon = 0.98$, and (a) $a/b = 3$, (b) $a/b = 2$, (c) $a/b = 1.5$. Solid lines: from Eq. (7). Dashed lines: cavity dynamics and spontaneous emission included.

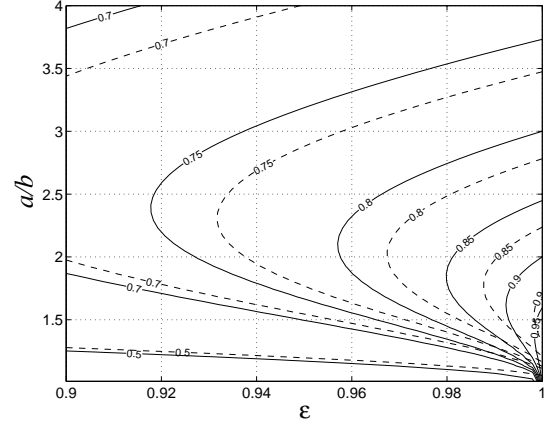


FIG. 4: Steady state fidelity as a function of ϵ and the ratio a/b . Other than Ω_r , Ω_t , and ϵ , the parameters are the same as in Fig. 3. Solid lines: from Eq. (7). Dashed lines: cavity dynamics and spontaneous emission included.

$a/b \rightarrow 1$. In fact, the slowest timescale in the atomic dynamics scales in proportion to $(a/b - 1)^{-2}$, which limits the maximum attainable fidelity once spontaneous emission is taken into account. As $a/b \rightarrow 1$ the scheme also becomes more sensitive to losses in transmission between the cavities (i.e., $\epsilon < 1$). This is highlighted by the fact that the solid curve for $a/b = 1.5$ lies below that for $a/b = 2$ (contrary to the ideal case when $\epsilon = 1$).

These features are illustrated further in the contour plot of Fig. 4, which shows the steady-state fidelity as a function of a/b and ϵ . Importantly, this plot also demonstrates that significant steady state entanglement is possible for relatively modest values of a/b and ϵ . Note in addition that the characteristic state preparation times

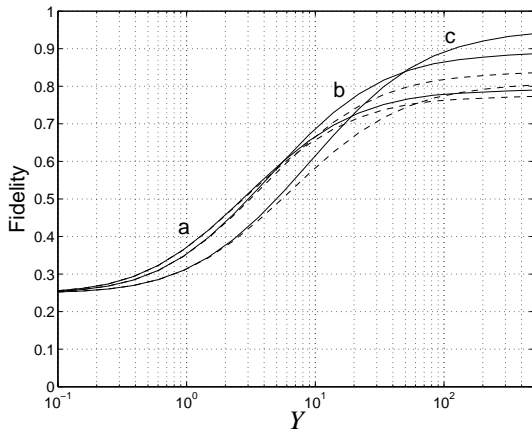


FIG. 5: Steady state fidelity versus $Y = g^2/(\kappa\gamma)$ for (a) $a/b = 3$, (b) $a/b = 2$, and (c) $a/b = 1.5$, with $\epsilon = 1$ (solid lines) and $\epsilon = 0.98$ (dashed lines). To obtain these curves, g is varied, while $\{\beta_{ri}, \beta_{si}\}$ are kept constant by adjusting $\{\Omega_{ri}, \Omega_{si}\}$ appropriately (so that the condition $\kappa \gg \beta_{ri}, \beta_{si}$ remains satisfied).

(see Fig. 3) are typically orders of magnitude smaller than achievable single atom trapping times (see, e.g., [26]).

A closer examination of rates associated with Eq. (7) and rates associated with atomic spontaneous emission ($\sim \gamma\Omega_j^2/\Delta_j^2$) shows that the effects of spontaneous emission can be obviated, for a particular value of a/b , with a sufficiently large value of $g^2/(\kappa\gamma)$. To quantify this more carefully, the steady state fidelity is plotted in Fig. 5 against the cooperativity parameter $Y = g^2/(\kappa\gamma)$ for several values of a/b and for two values of the coupling efficiency ϵ . The effects of spontaneous emission are clearly suppressed for $Y \gg 1$, although this condition becomes more demanding as $a/b \rightarrow 1$. However, it is also apparent from Fig. 5 (and Figs. 3 and 4) that for a particular $\epsilon < 1$ there exists an optimum value of a/b , greater than one, for which the achievable fidelity is maximized.

By breaking the symmetry between the two atoms with respect to Raman driving strengths (i.e., by varying the ratios β_{r1}/β_{r2} , β_{s1}/β_{s2} , as well as β_{r1}/β_{s1} and β_{r2}/β_{s2}), it is possible in principle to generate a wide variety of mixed entangled states, corresponding to most of the allowed combinations of entropy and concurrence [22, 27]. Given multiple atoms within each cavity and the ability to address these atoms individually and sequentially with laser fields, one might also contemplate the preparation of multiple pairs of entangled atoms, to which one could apply entanglement purification procedures [28]. Alternatively, with multiple atoms coupled collectively to the cavity mode at each site, it should be possible to prepare entangled states of separated atomic ensembles [18, 19, 20]. The collective enhancement of the atom-cavity coupling strength associated with many-atom systems would also alleviate the need for strong single-atom

cavity coupling strength (i.e., the condition $g^2/(\kappa\gamma) \gg 1$ would become $Ng^2/(\kappa\gamma) \gg 1$, where N is the number of atoms).

In conclusion, we have proposed a scheme for the unconditional steady-state preparation of entangled states of distantly separated atoms. The scheme does not require entangled light fields or projective measurements, and appears to be feasible with existing experimental parameters.

-
- [1] C. Monroe, *Nature* **416**, 238 (2002).
 - [2] H. Mabuchi and A. C. Doherty, *Science* **298**, 1372 (2002).
 - [3] J. I. Cirac, P. Zoller, H. J. Kimble, and H. Mabuchi, *Phys. Rev. Lett.* **78**, 3221 (1997).
 - [4] A. S. Parkins and E. Larsabal, *Phys. Rev. A* **63**, 012304 (2001).
 - [5] E. S. Polzik, *Phys. Rev. A* **59**, 4202 (1999).
 - [6] A. Kuzmich and E. S. Polzik, *Phys. Rev. Lett.* **85**, 5639 (2000).
 - [7] A. S. Parkins and H. J. Kimble, *Phys. Rev. A* **61**, 052104 (2000).
 - [8] K. Mølmer, *Opt. Commun.* **179**, 429 (2000).
 - [9] S. Lloyd, M. S. Shahriar, J. H. Shapiro, and P. R. Hemmer, *Phys. Rev. Lett.* **87**, 167903 (2001).
 - [10] M. D. Lukin, S. F. Yelin, and M. Fleischhauer, *Phys. Rev. Lett.* **84**, 4232 (2000).
 - [11] C. Cabrillo, J. I. Cirac, P. García-Fernández, and P. Zoller, *Phys. Rev. A* **59**, 1025 (1999).
 - [12] S. Bose, P. L. Knight, M. B. Plenio, and V. Vedral, *Phys. Rev. Lett.* **83**, 5158 (1999).
 - [13] X.-L. Feng *et al.*, *Phys. Rev. Lett.* **90**, 217902 (2003).
 - [14] L.-M. Duan and H. J. Kimble, *Phys. Rev. Lett.* **90**, 253601 (2003).
 - [15] C. Simon and W. T. M. Irvine, quant-ph/0303023.
 - [16] M. B. Plenio, D. E. Browne, and S. F. Huelga, quant-ph/0302185.
 - [17] A. Gilchrist, A. G. White, and W. J. Munro, *Phys. Rev. A* **66**, 012106 (2002).
 - [18] L.-M. Duan, J. I. Cirac, P. Zoller, and E. S. Polzik, *Phys. Rev. Lett.* **85**, 5643 (2000). Note that this scheme has been demonstrated experimentally by B. Julsgaard, A. Kozhekin, and E. S. Polzik, *Nature* **413**, 400 (2001).
 - [19] L.-M. Duan, M. D. Lukin, J. I. Cirac, and P. Zoller, *Nature* **414**, 413 (2001).
 - [20] L.-M. Duan, *Phys. Rev. Lett.* **88**, 170402 (2002).
 - [21] N. Lütkenhaus, J. I. Cirac, and P. Zoller, *Phys. Rev. A* **57**, 548 (1998).
 - [22] S. G. Clark and A. S. Parkins, *Phys. Rev. Lett.* **90**, 047905 (2003).
 - [23] C. W. Gardiner, *Phys. Rev. Lett.* **70**, 2269 (1993); H. J. Carmichael, *ibid.* **70**, 2273 (1993).
 - [24] P. Badziąg, M. Horodecki, P. Horodecki and R. Horodecki, *Phys. Rev. A* **62**, 012311 (2000).
 - [25] C. J. Hood *et al.*, *Science* **287**, 1447 (2000).
 - [26] J. McKeever *et al.*, *Phys. Rev. Lett.* **90**, 133602 (2003).
 - [27] M. Gu and A. S. Parkins, unpublished.
 - [28] W. Dür, H.-J. Briegel, J. I. Cirac, and P. Zoller, *Phys. Rev. A* **59**, 169 (1999).